Study on Spacecraft Attitude Determination with Nonlinear Filtering Algorithms

HUANG Lin[1], JING Wu-xing[2]
(1. R&D Center, DFH Satellite Company Ltd., Beijing 100094, China;
2. Dept. of Aerospace Engineering, Harbin Institute of Technology, Harbin 150001, China)

Abstract: The gyro-equipped spacecraft attitude determination from a sequence of vector observations is investigated in this paper. The spacecraft attitude determination is a nonlinear/non-Gaussian state filtering problem, so to use the classical filters proposed based on the extended Kalman filter (EKF) or unscented Kalman filter (UKF) might fail, especially when an accurate initial aprior state estimate is unexpectable. Recently the particle filtering algorithms have been applied to spacecraft attitude determination. However some algorithms need a large number of state particles. This is a heavy burden for the computers with limited capabilities. This paper is aimed to release the heavy burden by using dual-filter method, which temporally decomposed the attitude estimation from the rate gyro drift rate bias estimation at each iteration. Two novel filters including a modified dual particle filter (DPF) and a new hybrid filter (HF) are proposed. Both filters use a same quaternion particle filter which is a modification of a recently proposed algorithm, by using a slightly different resampling and regularizing algorithm. The DPF uses an auxiliary particle bias filter, whereas the HF uses a UKF bias filter. Various computer-based simulations are used to test the validity of the proposed novel filters and to compare them with several classical filters.

Key words: Attitude determination; Bayes estimation; Nonlinear filtering; Dual Filtering; Particle filtering
CLC number: V448.2　**Document code**: A　**Article ID**: 1000-1328(2010)12-2730-11
DOI: 10.3873/j.issn.1000-1328.2010.12.017

关于卫星姿态确定非线性滤波算法的研究

黄　琳[1]，荆武兴[2]
（1. 航天东方红卫星有限公司研发中心，北京 100094；
2. 哈尔滨工业大学，航天工程系，哈尔滨 150001）

摘　要：本文探讨了利用方位矢量和陀螺速率观测信息确定卫星姿态的问题。该问题实际上是一个非线性/非高斯状态滤波问题，因此，经典的基于 EKF 和 UKF 算法的姿态滤波器有可能失败，尤其是当初始状态的先验估计不可能精确得知的情况下。近来，粒子滤波理论已经开始应用于姿态确定问题，但是，这类算法往往需要大量的“粒子”，这对有限计算能力来说是一个沉重的负担。为此，本文尝试利用双重滤波方法，在每个序贯估计过程中，将有陀螺姿态确定问题暂时分解为 1 个四元数估计问题和 1 个陀螺常漂参数估计问题。本文提出了 2 个双重滤波器，包括 1 个姿态确定双重粒子滤波器和 1 个姿态确定的混合型滤波器。这两者都采用一个相同的四元数粒子滤波器，但在粒子重采样和平滑处理方面，不同于近来提出的类似滤波器。至于陀螺常漂估计，双重粒子滤波器发展了一个辅助粒子滤波器，而混合滤波器中则发展了一个参数 UKF 滤波器。通过与经典的姿态确定滤波器的仿真比较，证实了本文新提的 2 个算法的有效性和优越性。

关键词：姿态确定；贝叶斯估计；非线性滤波；双重滤波；粒子滤波

0　Introduction

Spacecraft attitude determination from a sequence of vector observations in gyro-equipped spacecraft has been intensively investigated and widely applied in practice[1-2]. The quaternion is a most popular attitude

收稿日期：2009-11-14；　修回日期：2010-07-27

representation for the global attitude estimation, though it is not a minimal representation because of its four dimensions. Various methods are proposed to keep the normalization constraint that has to be addressed in quaternion filtering problems. In general these methods can be classified as constrained estimation scheme and unconstrained estimation scheme[3-5]. The former scheme assumes the quaternion estimation error covariance matrix must be singular, and the central idea is to use a nonsingular representation (i. e., quaternion) for a reference attitude and a three-component representation for the deviations from the reference. The latter scheme assumes no such singularity and treats the four components of the quaternion as independent, but it has to incorporate some special normalization stages. More details about the two schemes and their advantages/disadvantages have been given in [3-5].

Nonlinear filtering algorithms have been used to estimate the quaternion and the gyro drift rate bias. Up to now, a number of attitude determination filters have been proposed, and some classical filters such as the multiplicative extended Kalman filter (MEKF[1]), the augmented extended Kalman filter (AEKF[6]), and the unscented Kalman quaternion filter (USQUE[7]) have been widely accepted. The MEKF and the USQUE are typical constrained estimation filters, which are brought forward based on the EKF algorithm and the UKF algorithm respectively. The AEKF is a typical unconstrained estimation filter which is proposed based on the EKF algorithm. Recently, the sequential Monte-Carlo algorithms or the particle filtering methods[8] have been applied to spacecraft attitude determination. Cheng and Crassidis proposed a particle filter to determine the modified Rodrigues parameter (MRP) and the drift rate bias[9]. However, the singularity associated with the MRP representation has to be addressed by frequently switching to an alternative set of MRPs or the quaternion, and also the ambiguity of the MRP has to be addressed by using a so-called ‘CONDMRP’ solution. Moreover, the six-dimensional particle filter has to simultaneously observe several vectors and use a huge number of particles (as many as 2000, an impractical computation burden for current onboard computers). As a result, the filter is not satisfied. A different estimator is proposed by Oshman and Carmi[10], which consists of a quaternion particle filter (QPF) and a genetic algorithm (GA) embedded gyro bias maximum-likelihood estimator. The QPF is a numerical unconstrained estimator which works directly with a number of weighted quaternion particles, and it is able to completely avoid the problem of singularity. This is a remarkable advantage over the Kalman filter variants, because they have to propagate and update the quaternion estimation error covariance matrix. The quaternion ambiguity problem has also been eliminated by using a special regularization method. The bias estimation is temporarily decoupled from the quaternion estimation at each iteration. Genetic algorithms are introduced to search an optimal bias estimate from a maximum likelihood cost function. The GA-embedded bias estimator is interlacing with the QPF, therefore the combined attitude determination filter is called by GA-QPF. The simulated results show this filter (even with 150 quaternion particles and a 200-element population for the bias estimator) can achieve a better performance with respect to several classical filters in the simulation cases where the initial quaternion estimate is uncertain. Nevertheless, the bias estimator seems sophisticated and over computing time consuming. Jiang et al propose a dual particle filter which includes an attitude particle filter and a bias particle filter[11]. The proposed attitude particle filter uses two attitude representations, the quaternion and the generalized Rodrigues parameter (GRP[12]). The quaternion is used for initial quaternion particle sampling, time propagating, observation updating, and particle resampling, while the GRP is used for the computations of the mean and the covariance matrix and the rougheing of the resampled particles. A similar idea has been given in [9] also. However, the GRP ambiguity problem has been ignored in [11]. The bias particle filter is the direct application of a standard particle filter (i. e., bootstrap filter). Jiang et al[13] proposed a marginalized particle filter for spacecraft attitude determination, by applying the Rao-Blackwellisation technique to an approximated quaternion and bias estimation, where the bias vector is partitioned from the augmented state of quaternion and bias and assumed to be conditionally linear Gaussian. Therefore the used bias estimator is a Kalman filter in nature. However, the model approximation of the original nonlinear/non-Gaussian attitude determination problems destroy the normalization constraint of the quaternion propagation, and its uncertain influence has not been considered and investigated. Once again, the GRP ambiguity problem has not been eliminated in this work.

This paper proposes two novel attitude determination filters for a low-Earth satellite with a three-axis magnetometer (TAM) and a three-axis gyro (TAG). The two filters are modified from the GA-QPF and the DPF[11]. Both filters take the QPF as their quaternion estimator, so that the frequent switching between the GRP and the quaternion is avoided for the particle attitude filter of [11], whereas the QPF given in this paper uses a slightly different quaternion particle resampling and regularizing methods. The main difference between the two filters is using different bias estimators. One filter uses an auxiliary particle filter, which is believed to be capable of resolving the state filtering problems with small process noise better than the bootstrap filter[8]. The other uses a UKF which is believed to be an appropriate algorithm for the gyro bias estimation of approximately Gaussian distribution and also for its low amount of calculation. Hence the two novel filters are named of the modified DPF and the HF respectively.

1 Gyro-equipped attitude determination state space models

A general continuous dynamics model is given in [1 - 2], which in general is discretized as[2,7]

$$\begin{bmatrix} \underline{\boldsymbol{q}}_{k+1} \\ \boldsymbol{\beta}_{k+1} \end{bmatrix} = \begin{bmatrix} \boldsymbol{\Phi}_{k+1,k}(\boldsymbol{\omega}_k)\, \underline{\boldsymbol{q}}_k \\ \boldsymbol{\beta}_k + \boldsymbol{\eta}_{u,k} \end{bmatrix} \tag{1}$$

where $\underline{\boldsymbol{q}}_k$ is the quaternion, $\underline{\boldsymbol{q}} = [\boldsymbol{q}^{\mathrm{T}} \quad q_4]^{\mathrm{T}}$, $\boldsymbol{q}$ is the vector part and q_4 is the scalar part. $\boldsymbol{\beta}_k$ is the TAG drift rate bias vector; $\{\boldsymbol{\eta}_{u,k}\}_{k=1}^{\infty}$ is a stationary zero-mean, white noise process with covariance $\sigma_u^2 \Delta t \boldsymbol{I}_{3\times 3}$, wherein $\Delta t = t_{k+1} - t_k$, $\boldsymbol{\Phi}_{k+1,k}(\boldsymbol{\omega}_k)$ is an orthogonal transition matrix about the true angular velocity $\boldsymbol{\omega}_k$ of the body (B) frame with respect to the reference (R) frame, ($\boldsymbol{\omega}_k$ is resolved in B frame.) and the matrix is given

$$\boldsymbol{\Phi}_{k+1,k}(\boldsymbol{\omega}_k) = \begin{bmatrix} \cos(0.5\|\boldsymbol{\omega}_k\|\Delta t)\boldsymbol{I}_{3\times 3} + \tilde{\boldsymbol{\omega}}_k & \tilde{\boldsymbol{\omega}}_k \\ -\tilde{\boldsymbol{\omega}}_k^{\mathrm{T}} & \cos(0.5\|\boldsymbol{\omega}_k\|\Delta t) \end{bmatrix} \tag{2}$$

the true rate $\boldsymbol{\omega}_k$ is unknown and is obtained from the TAG measurement, e. g., $\boldsymbol{\omega}_k = \tilde{\boldsymbol{\omega}}_k - \boldsymbol{\beta}_k - \boldsymbol{\eta}_{v,k}$ wherein $\tilde{\boldsymbol{\omega}}_k$ is the TAG measurement, $\boldsymbol{\eta}_{v,k}$ is the zero-mean white Gaussian measurement noise with covariance $\sigma_v^2 \boldsymbol{I}_{3\times 3}/\Delta t$, $\tilde{\boldsymbol{\omega}}_k = \sin(0.5\|\boldsymbol{\omega}_k\|\Delta t)\boldsymbol{\omega}_k/\|\boldsymbol{\omega}_k\|$. The TAM vector observation model is given[2]

$$\tilde{\boldsymbol{b}}_k = \boldsymbol{A}_k \boldsymbol{b}_{\mathrm{R},k} + \boldsymbol{v}_{\mathrm{B},k} \tag{3}$$

where $\tilde{\boldsymbol{b}}_k$ is the TAM measurement, $\boldsymbol{b}_{\mathrm{R},k}$ is the reference geomagnetic field, $\boldsymbol{v}_{\mathrm{B},k}$ is the TAM observation noise whose distribution is already known, $\boldsymbol{A}_k$ is the attitude matrix of the B frame with respect to the R frame and is the matrix representation of the quaternion $\underline{\boldsymbol{q}}_k$.

2 Modified dual particle filter

In this section, first the present quaternion particle filter which is slightly different from the QPF is simply introduced, then an auxiliary particle bias filter is completely given. Consider the resampling and regularizing disturb the posterior representation[8], it is better for the precision with a posterior estimation to implement the computations of the mean and the covariance before the resampling and regularizing stage.

2.1 Quaternion particle filter

2.1.1 Initialization ($k = 0$)

A single vector observation can not make the three-dimensional attitude completely observable, though the rest uncertain attitude information is reduced to one dimension, i. e., the rotation angle around the vector. Oshman and Carmi make use of the fact and propose a method to generate a number of initial quaternion particles (or samples) which keep the normalization constraint. A detailed technique is presented in Appendix B of [10]. However, the choice of an appropriate number of initial quaternion particles denoted by N_S depends on simulation experience. Denote the initial prior quaternion particle set by $\{\underline{q}_{0|-1}^i\}_{i=1}^{N_S}$ and the corresponding weight set by $\{\phi_{-1}^i\}_{i=1}^{N_S}$. Clearly, $\phi_{-1}^i = 1/N_S$.

2.1.2 Observation update ($k = 0, \cdots, N$)

Firstly calculate the likelihood probability of the quaternion particle $\underline{q}_{k|k-1}^i$,

$$L_k^i = \rho_v(\tilde{b}_k - A_k(\underline{q}_{k|k-1}^i)b_{R,k}),$$
$$i = 1, \cdots, N_S \tag{4}$$

where $\rho_v(\cdot)$ represents the probability density of the observation noise $v_{B,k}$.

Then calculate the weights $\{L_k^i \phi_{k-1}^i\}_{i=1}^{N_S}$ and normalize them as

$$\phi_k^i = \frac{L_k^i \phi_{k-1}^i}{\sum_{i=1}^{N_S} L_k^i \phi_{k-1}^i},\ i = 1, \cdots, N_S$$

2.1.3 Computation of mean and covariance ($k = 0, \cdots, N$)

The application of the classical solutions to compute the mean and the covariance from the weighted particle set to the weighted quaternion particles may destroy the normalization constraint and get in trouble with the quaternion ambiguity problem. One maximum posterior probability (MAP) approach and two minimum mean square error (MMSE) approaches are recommended in [10] to compute the mean quaternion. Consider a low accuracy of the MAP approach and the identical character of the two MMSE approaches, this paper only uses the second MMSE approach that is similar to Davenport's well known 'q-method'. The optimal quaternion estimate $\hat{\underline{q}}_{k|k}$ is the normalized eigenvector corresponding to the largest eigenvalue of matrix $K_{\hat{\underline{q}}}$

$$K_{\hat{\underline{q}}} \equiv \begin{bmatrix} B_k + B_k^T - I_{3\times3}\mathrm{tr}(B_k) & \zeta \\ \zeta^T & \mathrm{tr}(B_k) \end{bmatrix}$$

where tr(·) is operation of 'trace', matrix B_k and vector ζ are respectively defined by

$$B_k \equiv \sum_{i=1}^{N_S} \phi_k^i A_k(\underline{q}_{k|k}^i)$$

$$\zeta \equiv \begin{bmatrix} B_{k,23} - B_{k,32} \\ B_{k,31} - B_{k,13} \\ B_{k,12} - B_{k,21} \end{bmatrix}$$

The quaternion estimation error covariance is given[10]

$$P_{k|k}^{\underline{q}} = \sum_{i=1}^{N_S} \phi_k^i [\underline{q}_{k|k}^i \otimes \hat{\underline{q}}_{k|k}^{-1}][\underline{q}_{k|k}^i \otimes \hat{\underline{q}}_{k|k}^{-1}]^T$$

2.1.4 Resample and regularization ($k = 0, \cdots, N$)

Calculate the effective sample size $N_{\mathrm{eff}}^{\underline{q}}$

$$N_{\mathrm{eff}}^{\underline{q}} = \frac{1}{\sum_{i=1}^{N_S} (\underline{q}_{k|k}^i)^2}$$

If $N_{\mathrm{eff}}^{\underline{q}} < N_T^{\underline{q}}$ where $N_T^{\underline{q}}$ is given threshold (generally, $N_T^{\underline{q}} = 2N_S/3$), then resample the quaternion particles with the systematic resampling algorithm[8] and regularize the resampled particles with samples drawn from the Epanechnikov or Gaussian kernel[8]. The weights of the resampled particles are set to $1/N_S$. However a special regularization has to be used to eliminate the quaternion ambiguity. Inspired from the reference [10], a slightly different regularization is used.

Denote the 3 × 3 matrix of the vector part of the quaternion estimation error covariance $P_{k|k}^{\underline{q}}$ by $P_{k|k}^{q}$ and its square root matrix by $D_k = \sqrt{P_{k|k}^{q}}$, then draw samples as

$$\delta q_k^i = h_G D_k e_k^i,\ i = 1, \cdots, N_S$$

where e_k^i is sampled from a 3-dimensional zero-mean, unit covariance Gaussian kernel

$$e_k^i \sim N(e_k \mid 0, I_{3\times3}),\ i = 1, \cdots, N_S$$

wherein $N(\cdot \mid m, S)$ is a multivariate normal density with mean m and variance S; h_G is the bandwidth of the Gaussian kernel and is suggested with the optimal value

$$h_G = \left[\frac{4}{N_S(2n_{\underline{q}} + 1)}\right]^{1/(n_{\underline{q}}+4)}$$

wherein $n_{\underline{q}} = 4$. The deviation quaternion particles $\delta \underline{q}_k^i$ are obtained from

$$\delta \underline{q}_k^i \equiv \frac{[(\delta q_k^i)^T \quad 1]^T}{\sqrt{(\delta q_k^i)^2 + 1}},\ i = 1, \cdots, N_S$$

Finally, the diversity of the resampled quaternion particles is added as

$$\underline{q}_{k|k}^i = \delta \underline{q}_k^i \otimes \underline{q}_{k|k}^i,\ i = 1, \cdots, N_S$$

2.1.5 quaternion particle propagation ($k = 0,\cdots,N$)

The TAG sample period Δh is much smaller than the TAM sample period Δt. Assume the two periods satisfy $\boldsymbol{K}_{\mathrm{RIG}} = \Delta t/\Delta h$, where $\boldsymbol{K}_{\mathrm{RIG}}$ is an integer. The quaternion particle is propagated by using

$$\underline{\boldsymbol{q}}^i_{k+j+1|k+j} = \boldsymbol{\Phi}_{k+j+1,k+j}(\tilde{\boldsymbol{\omega}}_{k+j} - \hat{\boldsymbol{\beta}}_{k+j|k} - \boldsymbol{\eta}^i_{v,k+j}) \cdot \underline{\boldsymbol{q}}^i_{k+j|k+j-1},$$
$$i = 1,\cdots,N_s,\ j = 0,\cdots,K_{\mathrm{RIG}} - 1 \quad (5)$$

when $j = 0$, let $\underline{\boldsymbol{q}}^i_{k+j|k+j-1} = \underline{\boldsymbol{q}}^i_{k|k}$; when $j = K_{\mathrm{RIG}} - 1$, let $\underline{\boldsymbol{q}}^i_{k+j+1|k+j} = \underline{\boldsymbol{q}}^i_{k+1|k}$; $\tilde{\boldsymbol{\omega}}_{k+j}$ is the jth TAG measurement during the time interval $[t_k, t_{k+1}]$; $\hat{\boldsymbol{\beta}}_{k+j|k} = \hat{\boldsymbol{\beta}}_{k|k}$ where $\hat{\boldsymbol{\beta}}_{k|k}$ is the bias mean estimate given by the bias estimator, $\boldsymbol{\eta}^i_{v,k+j}$ is obtained from $N(\boldsymbol{\eta}_{v,k} \mid 0, \sigma_v^2 \boldsymbol{I}_{3\times3}/\Delta h)$. Note, the quaternion particle $\underline{\boldsymbol{q}}^i_{k+1|k}$ keeps the normalization constraint.

2.2 Auxiliary particle bias filter

Based on the standard particle filter (e. g., bootstrap filter), Pitt and Sheppard[14] proposed a so-called auxiliary particle filter that is able to automaticly generate particles from the particles of the previous time step which are most likely to the true state. Compared to the bootstrap filter, this filter is effective to deal with state filtering problems when the process noise is small. Consider that the process noise $\boldsymbol{\eta}_{u,k}$ is small for the bias vector $\boldsymbol{\beta}_k$, one can see the auxiliary particle filter is a better bias estimator.

2.2.1 Initialization ($k = 0$)

Draw initial aprior bias particles from the prior distribution $\rho(\theta_0)$, say, a Gaussian distribution

$$\boldsymbol{\beta}^i_{0|-1} \sim N(\boldsymbol{\beta}_0 \mid \hat{\boldsymbol{\beta}}_0, \boldsymbol{P}^\beta_0),\ i = 1,\cdots,N_P$$

where $\hat{\boldsymbol{\beta}}_0$ and $\boldsymbol{P}_0{}^\beta$ are the initial bias mean estimate and covariance estimate respectively. Denote the initial aprior bias particle set by $\{\boldsymbol{\beta}^i_{0|-1}\}^{N_P}_{i=1}$ and their corresponding weight set by $\{\varphi^i_{-1}\}^{N_P}_{i=1}$. Clearly, $\varphi^i_{-1} = 1/N_P$.
Calculate the initial likelihood probability

$$L^i_0 = \rho_v(\tilde{\boldsymbol{b}}_0 - \boldsymbol{A}_0(\underline{\boldsymbol{q}}^i_{0|-1})\boldsymbol{b}_{\mathrm{R},0}),\ i = 1,\cdots,N_P,$$

where the N_P initial quaternion particles $\{\underline{\boldsymbol{q}}^i_{0|-1}\}^{N_P}_{i=1}$ might be chosen from the generated initial quaternion particle set $\{\underline{\boldsymbol{q}}^i_{0|-1}\}^{N_S}_{i=1}$. Of course, this is for the case where $N_P \leqslant N_S$. Otherwise, the extra $N_P - N_S + 1$ quaternion particles $\{\underline{\boldsymbol{q}}^i_{0|-1}\}^{N_P}_{i=N_S+1}$ have to be additionally generalized. In this paper, assume $N_P = N_S$. Finally, calculate the weights $\{L^i_{0|-1}\varphi^i_{-1}\}^{N_P}_{i=1}$ and normalize them as

$$\varphi^i_0 = \frac{L^i_{0|-1}\varphi^i_{-1}}{\sum_{i=1}^{N_P} L^i_{0|-1}\varphi^i_{-1}},\ i = 1,\cdots,N_P$$

2.2.2 Bias particle propagation ($k = 1,\cdots,N$)

Firstly, calculate m^i_k which is characterization of $\boldsymbol{\beta}^i_{k|k-1}$, given from $\boldsymbol{\beta}^i_{k-1|k-1}$. This could be the mean or a sample written as

$$\boldsymbol{m}^i_k = \boldsymbol{\beta}^i_{k-1|k-1} + \boldsymbol{\eta}^i_{u,k-1},\ i = 1,\ \cdots,N_P$$

where $\boldsymbol{\eta}^i_{u,k-1} \sim N(0, \sigma_u^2 \Delta t \boldsymbol{I}_{3\times3})$.

Secondly, calculate the likelihood probability of some bias particle $\boldsymbol{m}^i_k$ by using a similar method as Eq. (4)

$$\Psi^i_k = \rho_v(\tilde{\boldsymbol{b}}_k - \boldsymbol{A}_k(\breve{\underline{\boldsymbol{q}}}^i_{k|k-1})\boldsymbol{b}_{\mathrm{R},k}),\ i = 1,\cdots,N_P$$

However $\breve{\underline{\boldsymbol{q}}}^i_{k|k-1}$ is obtained as follows

$$\breve{\underline{\boldsymbol{q}}}^i_{k-1+j+1|k-1+j} = \boldsymbol{\Phi}_{k-1+j+1,k-1+j}(\tilde{\boldsymbol{\omega}}_{k-1+j} - \boldsymbol{m}^i_k - \boldsymbol{\eta}^i_{v,k-1+j}) \cdot \breve{\underline{\boldsymbol{q}}}^i_{k-1+j|k-1+j-1},$$
$$i = 1,\cdots,N_S,\quad j = 0,\cdots,K_{\mathrm{RIG}} - 1 \quad (6)$$

when $j = 0$, let $\breve{\underline{\boldsymbol{q}}}^i_{k-1+j|k-1+j-1} = \hat{\underline{\boldsymbol{q}}}_{k-1|k-1}$ wherein $\hat{\underline{\boldsymbol{q}}}_{k-1|k-1}$ is the MMSE quaternion estimate, when $j = K_{\mathrm{RIG}} - 1$, let $\breve{\underline{\boldsymbol{q}}}^i_{k|k-1} = \breve{\underline{\boldsymbol{q}}}^i_{k-1+j+1|k-1+j}$, $\tilde{\boldsymbol{\omega}}_{k+j}$ is the j^{th} TAG measurement during the time interval $[t_{k-1}, t_k]$, $\boldsymbol{\eta}^i_{v,k-1+j} \sim N(0, \sigma_v^2 \boldsymbol{I}_{3\times3}/\Delta h)$. Since the vector observation equation (3) shows no direct correlation with the bias, the bias observation update is actually provided by the propagated quaternion particles, whereas the vector observation equation is more convenient for the computation of the likelihood probability than the quaternion prediction equation.

Thirdly, calculate the weights $\{\Psi^i_k \varphi^i_{k-1}\}^{N_P}_{i=1}$ and normalize them as

$$\psi^i_k = \frac{\Psi^i_k \varphi^i_{k-1}}{\sum_{i=1}^{N_P} \Psi^i_k \varphi^i_{k-1}},\ i = 1,\cdots,N_P$$

select the high likely bias particles of previous time step using the systematic resample method, e. g.,

$$[\{-,-,i^l\}^{N_P}_{l=1}] = \mathrm{RESAMPLE}[\{m^i_k, \psi^i_k\}^{N_P}_{i=1}]$$

where i^l represents the current particle 'l' is drawn from the particle 'i' of previous time step.

Finally, the bias particles are propagated as

$$\boldsymbol{\beta}^l_{k|k-1} = \boldsymbol{\beta}^{i^l}_{k-1|k-1} + \boldsymbol{\eta}^l_{u,k-1},\ l = 1, \cdots, N_P$$

where $\boldsymbol{\eta}^l_{u,k-1} \sim N(0, \sigma_u^2 \Delta t \boldsymbol{I}_{3\times3})$.

2.2.3 Observation update ($k = 1, \cdots, N$)

Firstly, calculate the likelihood probability again

$$\Psi^l_k = \rho_v(\tilde{\boldsymbol{b}}_k - \boldsymbol{A}_k(\breve{\underline{\boldsymbol{q}}}^l_{k|k-1})\boldsymbol{b}_{\mathrm{R},k}),\ l = 1, \cdots, N_P$$

where $\breve{\underline{\boldsymbol{q}}}^l_{k|k-1}$ is obtained by using a method similar to Eq. (6), whereas $\boldsymbol{\beta}^l_{k|k-1}$ is used instead of $\boldsymbol{m}^i_k$.

Then calculate the weights $\{\Psi^l_k/\Psi^{i^l}_k\}^{N_P}_{i=1}$ and normalize them as

$$\varphi^l_k = \frac{\Psi^l_k/\Psi^{i^l}_k}{\sum_{l=1}^{N_P} \Psi^l_k/\Psi^{i^l}_k},\ l = 1, \cdots, N_P$$

2.2.4 Computation of Mean and Covariance ($k = 0, \cdots, N$)

$$\hat{\boldsymbol{\beta}}_{k|k} = \sum_{l=1}^{N_P} \varphi^l_k \boldsymbol{\beta}^l_{k|k}$$

$$\boldsymbol{P}^{\beta}_{k|k} = \sum_{l=1}^{N_P} \varphi^l_k(\boldsymbol{\beta}^l_{k|k} - \hat{\boldsymbol{\beta}}_{k|k})(\boldsymbol{\beta}^l_{k|k} - \hat{\boldsymbol{\beta}}_{k|k})^{\mathrm{T}}$$

2.2.5 Resample and regularization ($k = 0, \cdots, N$)

This step is believed to be unnecessary for an auxiliary particle filter by Arulampalam et al[8], but improved by Pitt and Sheppard[14]. This paper suggests taking this step when the effective sample size N^{β}_{eff} is below given threshold, e. g., $2N_P/3$. The weights of the resampled bias particles are set to $1/N_P$. Regularize the resampled bias particles as follows

$$\boldsymbol{\beta}^l_{k|k} = \boldsymbol{\beta}^l_{k|k} + h_G \sqrt{\boldsymbol{P}^{\beta}_{k|k}}\boldsymbol{\varepsilon}^l_k,\ l = 1, \cdots, N_P$$

where $\sqrt{\boldsymbol{P}^{\beta}_{k|k}}$ is square root matrix; $\boldsymbol{\varepsilon}^l_k$ is sampled from a 3-dimensional zero-mean, unit covariance Gaussian kernel as

$$\boldsymbol{\varepsilon}^l_k \sim N(\boldsymbol{\varepsilon}_k \mid 0, \boldsymbol{I}_{3\times3}),\ l = 1, \cdots, N_P$$

3 Hybrid filter

The difference of the HF from the modified DPF is the use of a UKF bias estimator, which is a direct application of the UKF algorithm to the 3-dimensional bias estimation. The bias UKF is given as follows.

3.1 Initialization ($k = 0$)

Denote the initial aprior mean estimate and covariance estimate by $\hat{\boldsymbol{\beta}}_{0|-1} = \hat{\boldsymbol{\beta}}_0$ and $\boldsymbol{P}^{\beta}_{0|-1} = \boldsymbol{P}^{\beta}_0$. Use $\hat{\boldsymbol{\Theta}}_{0|-1}$ and $\boldsymbol{P}^{\Theta}_{0|-1}$ to generate a initial bias sigma point set $\{\boldsymbol{\beta}^i_{0|-1}\}^6_0$, the weights for calculating the mean and the covariance are denoted by $\{\omega^{m,i}_0\}^6_{i=0}$ and $\{\omega^{c,i}_0\}^6_{i=0}$ respectively.

Then choose seven initial aprior quaternion particles from the set $\{\boldsymbol{q}^i_{0|-1}\}^{N_S}_{i=1}$ and generate seven prediction observation sigma points as

$$z^i_0 = \boldsymbol{A}_0(\underline{\boldsymbol{q}}^i_{0|-1})\boldsymbol{b}_{\mathrm{R},0},\ i = 0, \cdots, 6$$

3.2 Observation update ($k = 0, \cdots, N$)

Firstly, calculate the mean observation

$$\hat{z}_k = \sum_{i=0}^{6} \omega^{(m,i)}_k z^i_k$$

Secondly, calculate the innovation and its covariance respectively

$$\boldsymbol{v}^{\beta}_k = z_k - \hat{z}_k$$

$$\boldsymbol{P}^{vv,\beta}_k = \sum_{i=0}^{6} \omega^{(c,i)}_k (z^i_k - \hat{z}_k)(z^i_k - \hat{z}_k)^{\mathrm{T}} + \boldsymbol{R}_k$$

where $\boldsymbol{R}_k$ is the covariance of the observation noise $\boldsymbol{\nu}_{\mathrm{B},k}$ which is regarded as a zero-mean, white Gaussian noise.

Thirdly, calculate the correlative covariance matrix and the gain matrix respectively

$$\boldsymbol{P}^{\beta z}_k = \sum_{i=0}^{6} \omega^{(c,i)}_k (\boldsymbol{\beta}^i_{k|k-1} - \hat{\boldsymbol{\beta}}_{k|k-1})(z^i_k - \hat{z}_k)^{\mathrm{T}}$$

$$\boldsymbol{K}^{\beta}_k = \boldsymbol{P}^{\beta z}_k(\boldsymbol{P}^{vv,\beta}_k)^{-1}$$

Finally, calculate the posterior mean and covariance respectively

$$\hat{\boldsymbol{\beta}}_{k|k} = \hat{\boldsymbol{\beta}}_{k|k-1} + \boldsymbol{K}^{\beta}_k \boldsymbol{v}^{\beta}_k$$

$$\boldsymbol{P}^{\beta}_{k|k} = \boldsymbol{P}^{\beta}_{k|k-1} - \boldsymbol{K}^{\beta}_k \boldsymbol{P}^{vv,\beta}_k (\boldsymbol{K}^{\beta}_k)^{\mathrm{T}}$$

3.3 Bias sigma point propagation ($k = 0, \cdots, N$)

Firstly predict the bias mean and the covariance matrix

$$\hat{\boldsymbol{\beta}}_{k+1|k} = \hat{\boldsymbol{\beta}}_{k|k}$$

$$\boldsymbol{P}^{\beta}_{k+1|k} = \boldsymbol{P}^{\beta}_{k|k} + \sigma_u^2 \Delta t \boldsymbol{I}_{3\times3}$$

Secondly, use $\hat{\boldsymbol{\beta}}_{k+1|k}$ and $\boldsymbol{P}^{\beta}_{k+1|k}$ to generate the aprior bias sigma point set $\{\boldsymbol{\beta}^i_{k+1|k}\}^6_0$, the weights for calculating the mean and the covariance are denoted by $\{\omega^{m,i}_{k+1}\}^6_{i=0}$ and $\{\omega^{c,i}_{k+1}\}^6_{i=0}$ respectively.

Then generate prediction observation sigma points as

$$z_{k+1}^{i} = A_{k+1}(\breve{q}_{k+1|k}^{i})b_{R,k+1}, i = 0, \cdots, 6$$

where

$$\breve{q}_{k+j+1|k+j}^{i} = \Phi_{k+j+1,k+j}(\tilde{\omega}_{k+j} - \beta_{k+1|k}^{i}) \cdot \breve{q}_{k+j|k+j-1}^{i},$$

$$i = 1, \cdots, 6, \quad j = 0, \cdots, K_{RIG} - 1$$

when $j = 0$, let $\breve{q}_{k+j|k+j-1}^{i} = \hat{q}_{k|k}$, where $\hat{q}_{k|k}$ is the MMSE quaternion estimate, when $j = K_{RIG} - 1$, let $\breve{q}_{k+1|k}^{i} = \breve{q}_{k+j+1|k+j}^{i}$, $\tilde{\omega}_{k+j}$ is the j^{th} TAG measurement during the time interval $[t_k, t_{k+1}]$.

4 Simulation results and analysis

A typical small satellite considered in [15] is chosen in the simulation section. The satellite runs in a nearly circular low Earth orbit with an inclination of 82° and a height of 823 km, it is out of control and spinning with an initial rate of 2.0°/s. The real geomagnetic field vector is simulated using a 10-order international geomagnetic reference field model. The reference vector is simulated using an 8-order model. White and colored TAM measurement noise processes are considered. The white Gaussian noise of 60 nT (σ) is used in the simulations of subsections 4.1 and 4.2, and the colored noise is introduced to the simulations of subsection 4.3. The colored-noise model is described by a first-order Markov process driven by white noise[16]. The 'time constant' of the Markov process has been chosen corresponding to an orbital arc length of 18° (about 300 s in this paper). The power spectral density of the white-noise driving term has been chosen, so that the magnitude of the colored noise will match the white Gaussian noise used in subsections 4.1 and 4.2. The measurements period Δt of the TAM is 10s. The TAG output is contaminated with a measurement noise with two components: a white zero-mean Gaussian process with intensity of $\sigma_v^2 = 0.1(\mu\text{rad})^2/\text{s}$ and a drift bias modeled as an integrated Gaussian white noise with intensity of $\sigma_u^2 = 1 \times 10^{-7}(\mu\text{rad})^2/\text{s}^3$. The true initial drift rate bias is set to 0.1 °/h on each axis. The sampling period Δh of the TAG is 1s.

4.1 Effects of various particle numbers on performances of the modified DPF and the HF

Various particle numbers are chosen to test the performances of the modified DPF and the HF. For convenience, let $N_P = N_S$. The initial bias mean estimate and the covariance estimate are given

$$\hat{\beta}_0 = [0.2°/\text{h} \quad 0.2°/\text{h} \quad 0.2°/\text{h}] \tag{7}$$

$$P_0^{\beta} = \text{diag}(0.4°/\text{h}, \quad 0.4°/\text{h}, \quad 0.4°/\text{h}) \tag{8}$$

To evaluate the quaternion and the bias filtering errors, two indexes used in [10] are introduced. One is for the quaternion estimation error (in degrees) evaluation and is given

$$\delta\alpha = 2\arccos(\delta q_4)$$

where δq_4 is the scalar component of the error quaternion $\delta \boldsymbol{q}$. The other is the TAG bias estimation error norm (in °/h).

The time histories of the quaternion estimation errors of four HF filters ($N_{SP} = 120$, $N_{SP} = 300$, $N_{SP} = 600$ and $N_{SP} = 900$) show the steady-state estimation errors are not more than 0.25° and the differences among them are slight. These HF filters converge from large initial errors (> 150°) into the steady-state errors in about 10min. Similar results are obtained from the modified DPF. However the bias estimation errors of the modified DPF filters and those of the HF filters shown in Fig. 1 are different. Fig. 1a shows the bias errors of the HF filters always remaining in the neighborhood of some constant bias during the whole time interval. Fig. 1b shows that the errors of the modified DPF filters first increasing and then remaining in the neighborhood of some constant bias. By far it is not difficult to find that the effects of particle numbers on the attitude and bias filtering performances of the two novel filters are not very crucial or clear when $900 \geq N_S = N_P \geq 120$. Therefore, in the following simulations, $N_S = N_P = 120$ are used.

In addition, a large initial bias estimate is used to test the convergent performance of the HF, e.g.,

$$\hat{\beta}_0 = [1.0°/\text{h} \quad 1.0°/\text{h} \quad 1.0°/\text{h}]$$

$$P_0^{\beta} = \text{diag}(1.0°/\text{h}, \quad 1.0°/\text{h}, \quad 1.0°/\text{h})$$

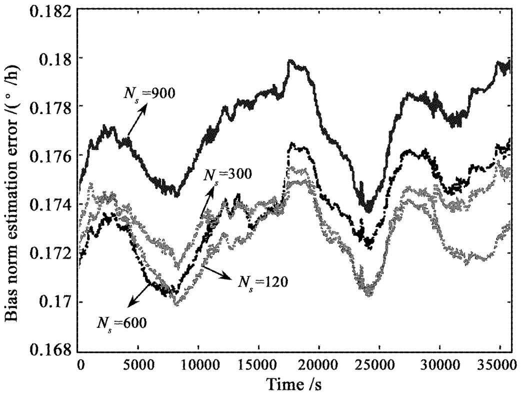

(a) HF

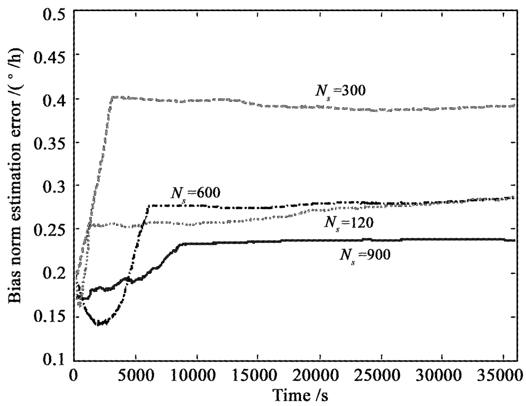

(b) Modified DPF

Fig. 1 Bias norm estimation errors of modified DPF and HF with various numbers of particle

However, it takes the HF about 11h to reach the steady-state attitude estimation error of 0.25°, and the bias norm estimation error indeed decreases to a nearly constant rate. As shown in Fig. 2, the slow rate does not mean the bias UKF is an inefficient filter in nature. The real reason, we suspect, is that the innovated information from the vector observations can not be directly fed back to the observation updating of the bias estimate. Unless mentioned, the initial bias estimate used in the simulations is better estimated as given in Eqs. (7) and (8).

4.2 Effects of initial quaternion estimate on filtering performances

The two novel filters have been compared to the MEKF and the USQUE. Different initial quaternion estimates have been considered for the MEKF and the USQUE, while the modified DPF and the HF generate the initial quaternion particles using the technique in Appendix B of[10].

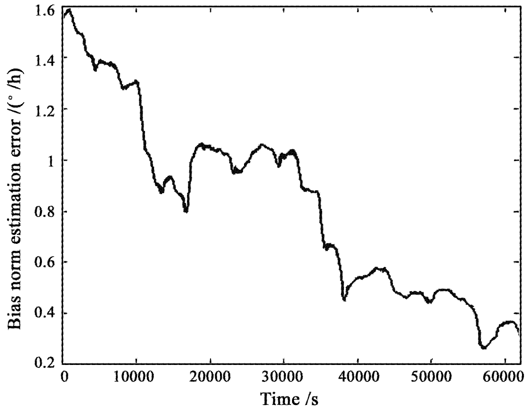

Fig. 2 Bias norm estimation errors of HF with a bad initial bias estimate

4.2.1 Constant initial quaternion of small estimation error

In this example, an initial quaternion estimate whose norm attitude error is 50° has been chosen for the MEKF and the USQUE. A large initial attitude covariance matrix has been chosen for the MEKF and the USQUE. Though the large matrix might be physically meaningless, it can speed up the convergence.

The results show that the four filters converge to the steady-state quaternion estimation errors at almost same rate and their quaternion estimation errors are of same level. However, the MEKF and the USQUE reach their bias estimation errors equivalent to HF in about 10000 s and the errors of all the three filters are lower than the modified DPF almost during the whole time interval, as shown in Fig. 3.

Obviously, the classical filters can achieve a better performance with much less calculation when the initial quaternion estimation error is small. If a good initialization is expectable, either the MEKF or the USQUE is a more promising filter.

4.2.2 Constant initial quaternion of large estimation error

In this example, a worse initial quaternion estimate whose norm attitude error is 160° has been chosen for the MEKF and the USQUE. Compared to those above results, the modified DPF and the HF keep almost same performances, whereas the performances of the other two classical filters sharply degenerate and

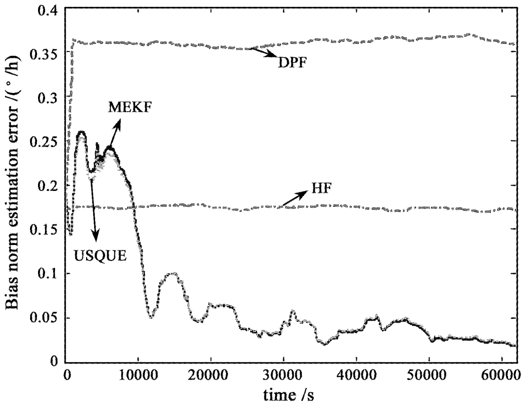

Fig. 3 Bias norm estimation errors of four filters with constant initial quaternion estimate (small-error case)

are much worse than the two novel filters. Fig. 4 shows that, the novel filters reach the quaternion estimation error of less than 0.25° in about 10 min, whereas the USQUE and the MEKF need about 17 h respectively to reach the errors of less than 0.5° and 1.5°. Obviously the modified DPF and the HF are more promising when the initial estimation error is large. Necessary to mention, the better performance of the USQUE with respect to that of the MEKF is obtained by regulating the UT parameter (i. e., $\alpha \in [0,1]$). That is to say, the same USQUE does not guaranteed in any case to achieve a steady performance than the MEKF. In other words, the classical filters depend more on the regulating work than the novel filters do.

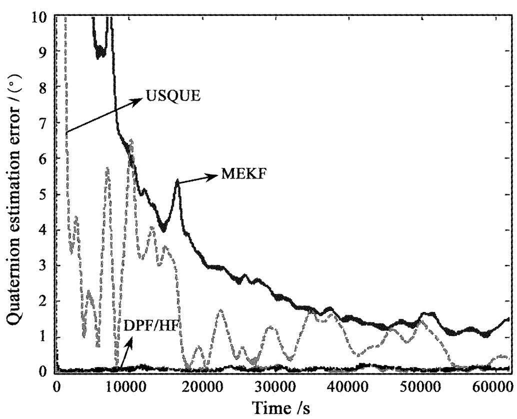

Fig. 4 Quaternion estimation errors of four filters with constant initial quaternion estimate (large-error case)

4.2.3 Uncertain initial quaternion

In this part, the initial quaternion estimates of the MEKF and the USQUE are ramdomly generated according to a uniform distribution on the unit hypersphere. The four filters are executed independently for 50 Monte Carlo runs. The maximum errors of the four filters during 30000 s to 62000 s are chosen for each run. The statistical distribution results of these maximum errors are given in Table 1. One can see that, the HF in 50 runs all reaches the quaternion estimation error of less than 0.5°. The convergent performance of the modified DPF is a little worse than HF but much better than the USQUE, The MEKF is the worst.

In addition, the average runtimes of the four filters are also tested. The results can be regarded as an indirect evaluation of their average calculation amounts. The 50 × 4 runs are executed in the computers of same computing capacity. If denote the average runtime of the MEKF as 1, then the USQUE, the HF, and the modified DPF are 6, 60, and 170 respectively. Surprisingly, the HF filter's runtime is only 10 times as the USQUE filter's. So the HF is a promising filter for onboard applications.

Table 1 Statistical distribution results of quaternion estimation errors of four filters with uncertain initial quaternion estimates (50 runs)

Filter	[0,0.5) /(°)	[0.5,1) /(°)	[1,2) /(°)	[2,180] /(°)
MEKF	64%	18%	12%	6%
USQUE	84%	8%	6%	2%
DPF	96%	4%	0%	0%
HF	100%	0%	0%	0%

4.3 Effects of colored observation noise on filtering performances

In this example, the performances of the four filters using colored TAM measurements have been tested. Use the third innovation (i. e., residual) component processes of the MEKF, the USQUE, the modified DPF, and the HF respectively for the white noise and the colored noise, an exact evaluation is done by computing the time-averaged autocorrelation[17]

$$\bar{\rho}_i(\bar{\lambda}) = \frac{1}{\sqrt{n_v}}\sum_{k=1}^{N_v} \boldsymbol{v}_{k,i}\boldsymbol{v}_{k+\bar{\lambda},i}\Big[\sum_{k=1}^{N_v}\boldsymbol{v}_{k,i}^2\sum_{k=1}^{N_v}\boldsymbol{v}_{k+\bar{\lambda},i}^2\Big]^{-1/2},$$

$$i = 1, 2, \cdots, n_v$$

where $\boldsymbol{v}_{k,i}$ is the i^{th} component of the innovation vector at time t_k; $\bar{\lambda}$ is the correlative step; n_v is the dimension of the innovation vector; N_v is the number of the considered observation data points. If the innovation process is zero-mean white Gaussian, the $\bar{\rho}_i(\bar{\lambda})$ is zero mean with variance of $1/N_v$ for N_v large enough. In this example, $N_v = 4000$ and various $\bar{\lambda}$ are used. The mean and variance results of $\bar{\rho}_i(\bar{\lambda})$ for the white noise and the colored noise are respectively given in Table 2 and Table 3. For an optimal filter, the mean and the variance of $\bar{\rho}_i(\bar{\lambda})$ should be 0 and 2.5×10^{-4} respectively. Table 2 shows that the mean results for the four filters are comparable and close to zero, whereas the variance results for the modified DPF and the HF are considerably close to the optimal values and the variance results for the two classical filters are far from the optimal values. That is, the novel filters can process the vector observations with white noise much better than the classical filters do. Similar conclusions can be drawn from the results shown in Table. 3. Comparing Table 3 to Table 2, one can see the variance values for the two novel filters which use the colored observations have increased many times, while those for the classical filters appear no remarkable varieties.

Table 2 Statistical results for time-averaged autocorrelation indexes of four filters' residuals (the third component) in the white-noise case

Filter	Mean			Variance		
	Axis x	Axis y	Axis z	Axis x	Axis y	Axis z
MEKF	-5.7×10^{-3}	-7.6×10^{-4}	1.7×10^{-2}	1.7×10^{-2}	2.1×10^{-2}	1.6×10^{-2}
USQUE	2.7×10^{-4}	9.5×10^{-3}	-6.5×10^{-4}	1.4×10^{-2}	8.9×10^{-3}	1.1×10^{-2}
DPF	-7.0×10^{-4}	3.4×10^{-3}	3.3×10^{-3}	6.9×10^{-4}	6.1×10^{-4}	5.3×10^{-4}
HF	-6.4×10^{-4}	4.4×10^{-3}	5.8×10^{-3}	5.7×10^{-4}	5.8×10^{-4}	5.0×10^{-4}

Table 3 Statistical results for time-averaged autocorrelation indexes of four filters' residuals (the third component) in the colored-noise case

Filter	Mean			Variance		
	Axis x	Axis y	Axis z	Axis x	Axis y	Axis z
MEKF	-4.4×10^{-3}	-9.3×10^{-3}	2.0×10^{-2}	1.8×10^{-2}	1.8×10^{-2}	1.6×10^{-2}
USQUE	-7.7×10^{-4}	9.1×10^{-3}	1.1×10^{-4}	1.4×10^{-2}	9.7×10^{-3}	8.7×10^{-3}
DPF	6.0×10^{-3}	1.5×10^{-3}	1.2×10^{-2}	3.1×10^{-3}	4.5×10^{-3}	3.4×10^{-3}
HF	5.5×10^{-3}	1.3×10^{-3}	9.0×10^{-3}	3.1×10^{-3}	4.7×10^{-3}	3.6×10^{-3}

5 Conclusions

Two novel filters are proposed for the gyro-equipped spacecraft attitude determination from vector observations. They are modified DPF and HF respectively. Both filters consist of same quaternion particle filter but use a different gyro drift rate bias estimator. The modified DPF filter uses an auxiliary particle bias filter, while the HF filter uses a UKF bias filter. An extensive simulation study has been done to evaluate the performances of the two novel filters and to compare them with two classical filters: the MEKF and the USQUE.

Several important conclusions are drawn. The first is, none of the considered filters can always achieve a best estimation performance in any case. The classical filters can achieve better estimation accuracy with respect to the two proposed novel filters with much smaller computing amounts when a good initial quaternion estimate is expectable; otherwise their convergent performances are possibly reduced and even much worse than those of the novel filters, whereas the proposed filters are able to achieve the consistent estimation performances in various cases. The second is, the effect of the particle number on the estimation performance of the modified DPF or the HF is not very crucial when the number is large enough. Surprisingly, both the HF and the modified DPF can achieve a better convergent performance with only 120 particles. The HF is a promising filter for the real-time spacecraft attitude determination applications. The third is, the novel filters can process the vector observations much better than the classical filters do. All considered filters show some certain robustness for colored vector observations. At last, an advice that has been made by someone else is repeated again, that is, the combined use of the classical Kalman filter variants and the recently proposed particle attitude determination filters is likely to achieve a better estimation performance. For example, the HF is used as an initialization stage for the MEKF or the USQUE.

References

[1] Lefferts E J, Markley F L, Shuster M D. Kalman filtering for spacecraft attitude estimation[J]. Journal of Guidance, Control, and Dynamics, 1982, 5(5): 417-429.

[2] Markley F L, Crassidis J L, Cheng Y. Nonlinear attitude filtering methods[C]. AIAA Guidance, Navigation, and Control Conf. and Exhibit, SA, California, USA, Aug., 2005.

[3] Shuster M D. Constraint in attitude estimation part I: constrained estimation[J]. The Journal of the Astronautical Sciences, 2003, 51(1): 51-74.

[4] Shuster M D. Constraint in attitude estimation part II: unconstrained estimation[J]. The Journal of the Astronautical Sciences, 2003, 51(1): 75-101.

[5] Markley F L. Attitude estimation or quaternion estimation[J]. The Journal of the Astronautical Sciences, 2004, 52(1-2): 221-238.

[6] Bar-Itzhack I Y, Oshman Y. Attitude determination from vector observations: quaternion estimation[J]. IEEE Trans. on Aerospace and Electric Systems, 1985, 21(1): 128-136.

[7] Crassidis J L, Markley F L. Unscented filtering for spacecraft attitude estimation[J]. Journal of Guidance, Control, and Dynamics, 2003, 26(4): 536-542.

[8] Arulampalam M S, Maskell S, Gordon N, Clapp T. A tutorial on particle filters for online nonliear/non-gaussian bayesian tracking [J]. IEEE Trans. On Signal Processing, 2002, 52(2): 174-188.

[9] Cheng Y, Crassidis J L. Particle filtering for sequential spacecraft attitude estimation[C]. AIAA Guidance, Navigation, and Control Conf. and Exhibit, Rhode Island, USA, Aug., 2004.

[10] Oshman Y, Carmi A. Attitude estimation from vector observation using genetic-algorithm-embedded quaternion particle filter[J]. Journal of Guidance, Control, and Dynamics, 2006, 29(4): 879-891.

[11] Jiang X Y, Ma G F. Spacecraft attitude estimation from vector measurements using particle filter[C]. The 4th Intel. Conf. on Machine Learning and Cybernetics, Guangzhou, China, Aug., 2005.

[12] Schaub H, Junkins J L. Stereographic orientation parameters for attitude dynamics: a generalization of the rodrigues parameters[J]. The Journal of the Astronautical Sciences, 1996, 44(1): 1-19.

[13] Jiang X Y, Ma G F. Satellite attitude estimation based on marginalized particle filter[J]. Control and Decision, 2007, 22(1): 39-44.

[14] Pitt M, Shephard N. Filtering via simulation: auxiliary particle filters[J]. J. Amer. Statist. Assoc., 1999, 94(446): 590-599.

[15] Psiaki M L. Global magnetometer-based spacecraft attitude and rate estimation[J]. Journal of Guidance, Control, and Dynamics, 2004, 27(2): 240-250.

[16] Alonso R, Shuster M D. TWOSTEP: a fast robust algorithm for attitude-independent magnetometer-bias determination[J]. The Journal of the Astronautical Sciences, 2002, 50(4): 433-451.

[17] Bar-Shalom Y, Li X R, Kirubarajan T. Estimation with applications to Tracking and Navigation[M]. New York: John Wiley & Sons, Inc., 2001.

Huang Lin(1979-), Dr Huang is a system engineer of DFH satellite company Ltd., the working area includes small system design, spacecraft GNC, and nolinear filtering.
Address: P. O. Box 9616, 100086 Beijing, China
Tel: (010)68744245-211
E-mail: doudou-huang@sohu.com

（编辑:曹亚君）